

AD-A121 267

NUMERICAL STUDY OF PHASE CONJUGATION IN STIMULATED  
BACKSCATTER WITH PUMP DEPLETION(U) NAVAL RESEARCH LAB  
WASHINGTON DC R H LEHMBERG 17 SEP 82 NRL-MR-4890

171

UNCLASSIFIED

SBI-AD-E000 503

F/G 20/5

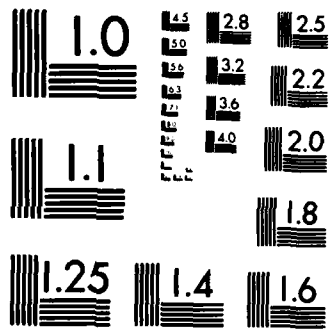
NL



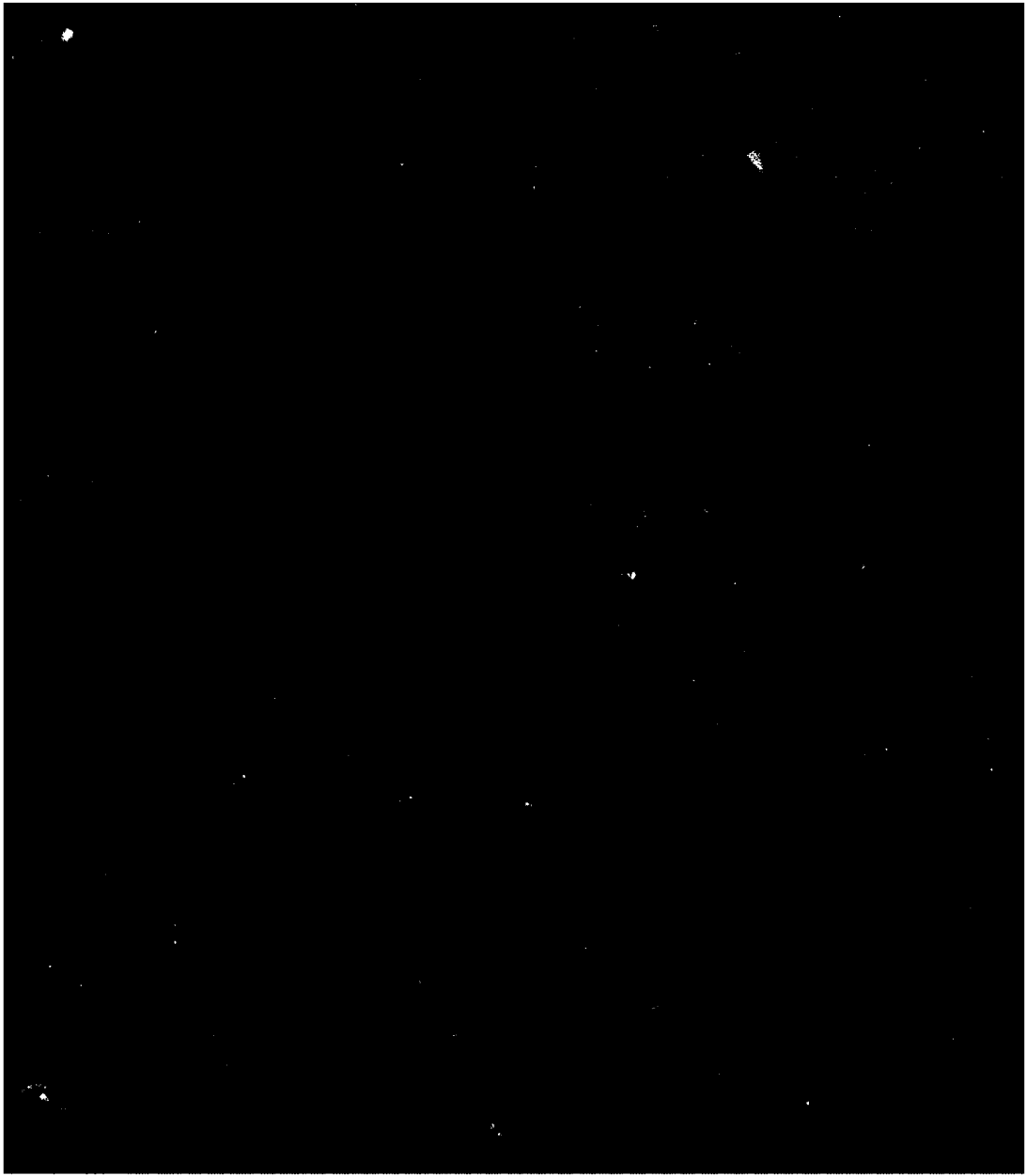
END

FILED

DTIC



MICROCOPY RESOLUTION TEST CHART  
NATIONAL BUREAU OF STANDARDS-1963-A





## CONTENTS

I.	INTRODUCTION .....	1
II.	THEORY AND CODE DESCRIPTION .....	1
III.	RESULTS .....	3
IV.	DISCUSSION .....	4
	ACKNOWLEDGMENT .....	5
	REFERENCES .....	5

**S** **DTIC**  
**ELECTE** **D**  
 NOV 3 1982  
**B**



Accession For	
NTIS GRA&I	<input checked="" type="checkbox"/>
DTIC TAB	<input type="checkbox"/>
Unannounced	<input type="checkbox"/>
Justification	
By	
Distribution/	
Availability Codes	
Avail and/or	
Dist	Special
<b>A</b>	

# NUMERICAL STUDY OF PHASE CONJUGATION IN STIMULATED BACKSCATTER WITH PUMP DEPLETION

## I. INTRODUCTION

Optical wavefront reversal or phase conjugation in stimulated backscatter has been the subject of extensive experimental<sup>1-13</sup> and theoretical<sup>14-22</sup> investigation over the last ten years. Most of the experiments are either of the aberration correction (ABC) type,<sup>1-9</sup> in which the conjugate backscatter reverses phase distortion induced on the incident beam by an aberrator, or the image replication (IMR) type,<sup>10-13</sup> in which the backscatter retraces an image formed by a mask (with or without an aberrator) in the incident beam. The ABC experiments normally record only the far field of the aberrator, whereas the IMR experiments observe at a point conjugate to the mask. Although the existing analytic theories<sup>14-20</sup> can explain how a phase conjugate wave is generated in stimulated backscatter, they have made no attempt to actually model these experimental configurations; nor have they realistically included pump depletion, which becomes important when the backscatter is significantly above threshold.<sup>1,7,9,13</sup> (One analytic treatment has included pump depletion,<sup>21</sup> but its assumptions and limitations are not applicable to the conditions studied here.)

In an earlier paper,<sup>22</sup> image replication in stimulated Brillouin scattering (SBS) of coherent beams was studied numerically, using a steady state 2D propagation code (BOUNCE). The present work treats phase conjugation of a focused *aberrated* beam, using a modified version of BOUNCE that has been extended to include pump depletion. In all of the cases studied, pump depletion significantly enhanced the fidelity of the phase conjugation process by inhibiting spatial gain narrowing. The simulations show that the far field distribution of light scattered back through the phase aberrator exhibits a prominent axial spike closely matching that of the incident beam, in agreement with the ABC experiments. However, the *near* field intensity exhibits large and rapid spatial inhomogeneities, even when the conjugation fidelity approaches 90%. In spite of such structure, the backscatter was able to reproduce a rough image of large scale intensity modulation imposed upon the incident beam; i.e., the results can simulate even those IMR experiments in which phase aberration was also present.<sup>10,11</sup>

## II. THEORY AND CODE DESCRIPTION

Under steady state conditions, the complex pump and SBS backscatter amplitudes  $E_L(x,z)$  and  $E_S(x,z)$  satisfy the parabolic equations

$$\left( \frac{\partial}{\partial z} + \frac{i}{2k} \frac{\partial^2}{\partial x^2} \right) E_L = \frac{1}{2} g |E_S|^2 E_L \quad (1a)$$

$$\left( \frac{\partial}{\partial z} - \frac{i}{2k} \frac{\partial^2}{\partial x^2} \right) E_S = \frac{1}{2} g |E_L|^2 E_S \quad (1b)$$

in a two dimensional cartesian geometry. Here,  $k = 2\pi n/\lambda$  is the magnitude of the propagation vectors (assumed equal for the two waves),  $x$  is the transverse coordinate, and  $g$  is the coupling coefficient of the Brillouin medium, which is contained within a region  $z_1 \leq z \leq z_2$ . BOUNCE solves Eqs. (1), assuming the aberrated pump wave is incident at  $z_2$ , while the backscatter grows from a small counter-propagating noise wave  $E_S(x,z_1)$  introduced at  $z_1$ . (E.g., see Fig. 1.) Both waves are assumed to vanish

at (and near) the transverse boundaries  $\pm X/2$ . The calculations were carried out using a grid of  $512 \times 200$  points.

Except for the inclusion of pump depletion, the present version of BOUNCE is similar to the one described in Ref. (22). (The only other major difference is that the predictor-corrector algorithm has been replaced by a split operator technique<sup>23</sup> in order to decrease the running time.) The inclusion of pump depletion is a nontrivial problem, however, because the two coupled waves are incident on opposite sides of the Brillouin medium, and neither one is known within that medium at the outset. One must know  $E_S(x,z)$  in order to calculate  $E_L(x,z)$ , and vice versa. The brute force solution would be to simply integrate the time dependent equations over many optical transits across the medium until steady state is finally attained. The approach followed here is a modified iteration procedure, which is significantly faster. Basically, it starts with an undepleted pump wave  $E_L^{(1)}(x,z)$ , calculates the resultant backscatter  $E_S^{(1)}(x,z)$  throughout the medium, then alternately recalculates these waves until the solutions converge to self consistency. This procedure must be supplemented by stabilization techniques in order to achieve that convergence. Acting alone, it would produce solutions that oscillate between two extremes, even when the incident pump amplitude is "turned on" gradually over many iterations.

The primary stabilization technique is based on the fact that the correct steady state solutions must satisfy the energy conservation relation,

$$P_L(z) - P_S(z) = P_L(z_1) - P_S(z_1) \approx P_L(z_1), \quad (2)$$

where

$$P_\alpha(z) = \int_{-X/2}^{X/2} |E_\alpha(x,z)|^2 dz \quad (3)$$

is proportional to the total power of the pump ( $\alpha = L$ ) or backscatter ( $\alpha = S$ ) at  $z$ . Expression (2) follows immediately from (1a,b) and the stated boundary conditions at  $\pm X/2$ . The actual stabilizing technique then consists of multiplying the coupling coefficient  $g$  in Eqs. (1a,b) by the factor  $1 + \gamma F(z) - \gamma$ , where

$$F(z) = \frac{P_L(z) - P_S(z)}{P_L(z_1)} \approx \frac{P_L(z) - P_S(z)}{P_L(z_1) - P_S(z_1)} \quad (4)$$

and  $\gamma$  is a positive bias factor of order  $3 \leq \gamma \leq 6$ . Thus, if  $|E_S(x,z_1)|^2$  starts to become too large, it automatically limits itself by reducing the growth rate  $1/2(1 + \gamma F - \gamma)g|E_L|^2$  in Eq. (1b). A similar restraint prevents excessive depletion of the counterpropagating pump wave in Eq. (1a). When the iterations finally converge to steady state,  $F$  approaches unity throughout the medium, so the bias becomes inoperative. In a one dimensional test problem, this technique worked well in all cases, giving the well known steady state solutions<sup>24</sup> to a high degree of accuracy. In two dimensions, however, it failed to completely stabilize for reflectivities  $> 15\%$ , and therefore had to be supplemented by an additional technique.

The second technique performs a weighted average of the calculated intensities with those of the previous iteration. In the  $m$ th iterative solution of Eq. (1a), one first calculates  $|E_L^{(m)}(x,z)|^2$ , then makes the replacement

$$|E_L^{(m)}(x,z)|^2 \rightarrow 1/2 [|E_L^{(m)}(x,z)|^2 + |E_L^{(m-1)}(x,z)|^2 P_L^{(m)}(z)/P_L^{(m-1)}(z)] \quad (5a)$$

at each point when  $m \geq 2$ . A similar replacement is performed when solving (1b):

$$|E_S^{(m)}(x,z)|^2 \rightarrow 1/2 [|E_S^{(m)}(x,z)|^2 + |E_S^{(m-1)}(x,z)|^2 P_S^{(m)}(z)/P_S^{(m-1)}(z)] \quad (5b)$$

These averages have the important property that they leave the integrals  $P_L^{(m)}(z)$  and  $P_S^{(m)}(z)$  invariant, and therefore do not interfere with the primary stabilization. With this combination of techniques, the solutions typically converge to self consistency within 15 to 20 iterations. Best results were obtained when the incident  $E_L^{(m)}(x,z_1)$  was turned on gradually over the first 5 to 10 iterations.

In addition to calculating the pump and backscatter profiles, BOUNCE also evaluates the average intensity gain  $G_I = \langle |E_S|^2 \rangle_{z_2} / \langle |E_S|^2 \rangle_{z_1}$ ,<sup>22</sup> total reflectivity  $R = P_S(z_2)/P_L(z_2)$ , and the normalized correlation function

$$H(z) = \frac{1}{P_L(z)P_S(z)} \left| \int_{-X/2}^{X/2} E_L(x,z) E_S(x,z) dx \right|^2, \quad (6)$$

which measures the phase conjugate fidelity. (Note that  $H = 1$  in the case of perfect conjugation,  $E_S \propto E_L^*$ .) From Eqs. (1a,b) and the boundary conditions at  $\pm X/2$ , one can readily verify that  $H$  remains constant when  $g = 0$ ; thus,  $H = H(z_2)$  at all points beyond the Brillouin medium.

### III. RESULTS

Figure 1, which corresponds to the case of negligible pump depletion, models a typical aberration compensation experiment, and illustrates several general features of the simulations presented in this paper. A coherent hyper-Gaussian pump beam of  $\lambda = 694$  nm traverses the aberration plate A, which imposes a random phase modulation and concomitant  $\sim 6$  mrad angular divergence ( $\sim 25 \times$  diffraction limit) shown in Fig. 2. A 6 cm lens then focuses the aberrated beam at the center of a 2 cm thick Brillouin medium. In all of these simulations, the noise source at  $z_1$  was modelled by a random complex field  $E_S(x,z_1)$  of 250 mrad angular divergence, giving typical pump-noise correlations  $H(z_1) \approx 0.1\%$ . However, the phase conjugate behavior of the backscatter was found to be generally insensitive to the statistical properties of the noise source (including even a *coherent* source) as long as  $H(z_1)$  remained small.

Referring again to Fig. 1, we see that as  $E_S(x,z)$  propagates toward  $z_2$ , it develops an inhomogeneous intensity distribution similar to the center portion of  $|E_L(x,z)|^2$ . This tendency of the pump beam to pull the backscattered radiation toward the strong central region (i.e., spatial gain narrowing) has been noted earlier,<sup>15,16,19,22</sup> and appears to be the main reason for the lower conjugate fidelities found in focused experiments.<sup>4-7</sup> In the example shown here,  $H = 61\%$ .

From  $z_2$ , the backscatter retraces the pump path through the lens and aberrator to produce the near and far field intensity profiles shown on the right hand side of Fig. 1. The phase compensation is evident in the far field, where the backscatter exhibits a strong central spike that closely matches the angular spectrum of the unaberrated incident beam. The  $\sim 40\%$  unconjugated component appears mainly as low level sidelobes and background hash; hence, expression (6) gives

$$H \approx \frac{\text{backscatter power in the central spike}}{\text{total backscatter power}}. \quad (7)$$

From a rough estimate of the total background energy shown in the figure, one obtains  $1 - H \approx 30\%$ , with the remaining 10% presumably accounted for by the slight broadening of the central spike, plus residual hash lying outside the  $\pm 4$  mrad interval or too small to be seen. Although the peak levels of the background are only a few percent of the on-axis intensity, they are still significantly larger than the experimentally observed values.<sup>4-7</sup> This stems from the fact that the hash is confined to only one transverse dimension; i.e. it lacks the usual geometrical weighting factor that would require much lower levels in the analogous two dimensional "halo" in order to satisfy expression (7).

In the near field of the aberrator, the conjugated and unconjugated components become mixed, resulting in serious degradation of the entire profile. This behavior, which was found in all cases, has gone largely unnoticed in the aberration correction experiments, since these generally record only *far* field intensities. It will be discussed in greater detail in Sec. IV.

Additional calculations were carried out with the same configuration to determine how the performance was affected by the gain  $G_I$  in the absence of pump depletion. The resulting beam profiles and

correlations were similar to those shown in Fig. 1. The fidelity exhibited a maximum value  $H_{\max} \approx 64\%$  around  $G_I \approx e^{13}$ , and decreased gradually to 55% at  $G_I \approx e^{25}$ .

The effect of pump depletion was studied by increasing the average noise and pump intensities, while holding the gain approximately constant around  $e^{17}$ .<sup>\*</sup> Under these conditions, the fidelity improved monotonically with reflectivity  $R$ ; e.g., the simulations gave  $H = 68\%$  at  $R = 10\%$ ,  $H = 76\%$  at  $R = 24\%$ , and  $H = 84\%$  at  $R = 47\%$ . Figure 3 shows the beam profiles for the last case. The reason for the improvement is evident from a comparison of the  $z_2$  plots in Figs. 1 and 3; i.e., the large backscatter tends to counteract spatial gain narrowing by selectively depleting the more intense center portion of the pump beam at  $z < z_2$ . These results are in qualitative agreement with a recent experimental study by Mays and Lysiak,<sup>7</sup> which reported a steady improvement in fidelity with increasing incident power well above threshold. The improvement was especially evident in the case where there were no reflections from the walls of the Brillouin cell, and hence where gain narrowing effects were most important. (In two other experiments,<sup>6,9</sup> the fidelity was found to deteriorate with increasing incident power; however, these experiments were carried out under conditions where self focusing is likely to have dominated within the cell.)

Although the enhanced fidelity significantly reduces the background hash, and narrows the axial spike at the far field (as one would expect from expression (7)), it results in only a partial improvement in the near field beam quality at the aberrator. Figure 4 shows that in spite of the persistent small scale inhomogeneities, the backscatter can still retrace *gross* features imposed upon the incident beam. This result is consistent with the image replication experiment of Ref. (11), in which an aberrator was present in addition to the mask. It is interesting to note from the  $z_2$  plot that the effect does not require an image of the structure to be maintained within the Brillouin medium.

In all of the simulations presented here, the aberrator was modelled using the same statistical realization. Other realizations yielded different values of  $H$  and differences in detailed structure of the profiles; however, the trends and general appearance of the profiles remained unchanged. In particular, the poor beam quality at the aberrator was found in all cases, even one for which the fidelity was 88%.

#### IV. DISCUSSION

Several of the results presented in Sec. III were not unexpected; e.g., the enhancement of fidelity by the pump depletion was suggested earlier by qualitative theoretical arguments.<sup>15,19,22</sup> However, the consistently poor beam quality of the backscatter at the aberrator, even for  $H \approx 90\%$ , deserves some additional comment. This behavior can be adequately explained if one approximates the pump and backscatter amplitudes at the right hand side of the aberrator by

$$E_L \approx \text{constant} \quad (8a)$$

$$E_s(x) \approx R^{1/2} E_L \left[ 1 + \sum_{N \neq 0} \alpha_N \exp(2\pi i N x / D) \right] \quad (8b)$$

within the interval  $-D/2 \leq x \leq D/2$ , and zero outside. The mode amplitude can then be written as  $\alpha_N = E_{SN}/E_{S0}$ , where  $E_{S0}$  and  $E_{SN}$  are, respectively, the peak far field amplitudes of the central spike and the  $N$ th lobe at angle  $N\lambda/D$ . Substituting Eqs. (8a,b) into (6), one obtains

$$H \approx \left[ 1 + \sum_{n \neq 0} |\alpha_n|^2 \right]^{-1} \quad (9)$$

which is consistent with expression (7) if all lobes are of equal width. For  $M$  modes of equal RMS amplitude  $\alpha_{RMS}$ , the fidelity is  $H \approx (1 + M\alpha_{RMS}^2)^{-1}$  while the fractional fluctuation of  $|E_s(x)|^2$  is of order  $\pm 2M^{1/2} \alpha_{RMS}$  (assuming  $2M^{1/2} \alpha_{RMS} < 1$  and  $\alpha_{RMS}^2 \ll 1$ ). For the simulation shown in Fig. 3, we estimate  $M \approx 10$  and  $\alpha_{RMS}^2 \approx 0.01$ , obtaining  $H \approx 91\%$  with 4:1 intensity variations at the aberrator. It is instructive to note that even a 99% fidelity would result in  $\pm 20\%$  variations.

The simulations presented in this paper have shown the importance of pump depletion and spatial gain narrowing on phase conjugation in focused SBS experiments, and illustrated the problem of near field beam quality. A modified version of the numerical techniques described here can also be used to model an optical waveguide Brillouin mirror, or a degenerate four wave mixing geometry in the limit of small beam crossing angles.

#### ACKNOWLEDGMENT

The author wishes to thank John McMahon, Peter Ulrich, and Harvey Brock for their valuable discussions. This work was supported jointly by the Office of Naval Research and the U.S. Department of Energy.

#### REFERENCES

1. B. Ya. Zel'dovich, V.I. Popovichev, V.V. Ragul'skii, and F.S. Faizullov, *Pis. Zh. ETF* **15**, 160 (1972) [Translation: *JETP Lett.* **15**, 109 (1972)].
2. B. Ya. Zel'dovich, N.A. Mel'nikov, N.F. Pilipetskii, and V.V. Ragul'skii, *Pis. Zh. ETF* **25** 41 (1977) [Translation: *JETP Lett.* **25**, 36 (1977)].
3. V.N. Blashchuk, et al., *Pis. Zh. Tekh. Fiz.* **3**, 211 (1977) [Translation: *Sov. Tech. Phys. Lett.* **3**, 83 (1977)].
4. V. Wang and C.R. Giuliano, *Opt. Lett.* **2**, 4 (1978).
5. C.R. Giuliano, et. al., *Correction of Phase Distortion by Nonlinear Optical Techniques*, Hughes Research Laboratories Interim Technical Report for period 15 July 1977 - 30 September 1978 (March 1979).
6. N.G. Basov, et al., *Kvant. Elektron.* **6**, 765 (1979) [Translation: *Sov. JQE* **9**, 455 (1979)].
7. R. Mays, Jr. and R.J. Lysiak, *Optics Comm.* **32**, 334 (1980).
8. N.F. Pilipetskiy, V.I. Popovichev, and V.V. Ragul'skiy, *Optics Comm.* **40**, 73 (1981).
9. M.C. Gower and R.G. Caro, *Opt. Lett.* **7**, 162 (1982).
10. K. Eidmann and R. Sigel, *Laser Interaction and Related Plasma Phenomena*, ed. by H.J. Schwarz and H. Hora (Plenum, New York, 1974) Vol. 3B.
11. V.I. Bespalov, A.A. Betin, and G.A. Pasmanik, *Pis. Zh. Tekh. Fiz.* **3**, 215 (1977) [Translation: *Sov. Tech. Phys. Lett.* **3**, 85 (1977)].
12. A.I. Sokolovskiyaya, G.L. Blekhovskikh, and A.D. Kudryavtseva, *Optics Comm.* **24**, 74 (1978).
13. M. Slatkine, I.J. Bigio, B.J. Feldman, and R.A. Fisher, *Opt. Lett.* **7**, 108 (1982).
14. V.G. Sidorovich, *Zh. Tekh. Fiz.* **46**, 2168 (1976) [Translation: *Sov. Phys. Tech. Phys.* **21**, 1270 (1976)].

---

\*This value was chosen because it became more difficult to stabilize the iteration procedure at higher gains.

15. N.B. Baranova, B. Ya. Zel'dovich, and V.V. Shkunov, *Kvant. Elektron.* **5**, 973 (1978) [Translation: *Sov. JQE* **8**, 559 (1978)].
16. N.B. Baranova and B. Ya. Zel'dovich, *Kvant. Elektron.* **7**, 973 (1980) [Translation: *Sov. JQE* **10**, 555 (1980)].
17. R.W. Hellwarth, *J. Opt. Soc. Am.* **68**, 1050 (1978).
18. R.W. Hellwarth, *Opt. Eng.* **21**, 263 (1982).
19. R.H. Lehmberg and B.H. Ripin, *Proc. of the International Conference on Lasers '78*, ed. V.J. Corcoran (STS Press, McLean, VA, 1979).
20. B. Ya. Zel'dovich and T.V. Yakovleva, *Kvant. Elektron.* **8**, 314 (1981) [Translation: *Sov. JQE* **11**, 186 (1981)].
21. G.G. Kochemasov and V.D. Nikolaev, *Kvant. Elektron.* **6**, 1960 (1979) [Translation: *Sov. JQE* **9**, 1155 (1979)].
22. R.H. Lehmberg and K.A. Holder, *Phys. Rev. A* **22**, 2156 (1980).
23. J.A. Fleck, Jr., J.R. Morris, and M.D. Feit, *Appl. Phys.* **10**, 129 (1976).
24. C.L. Tang, *J. Appl. Phys.* **37**, 2945 (1966).

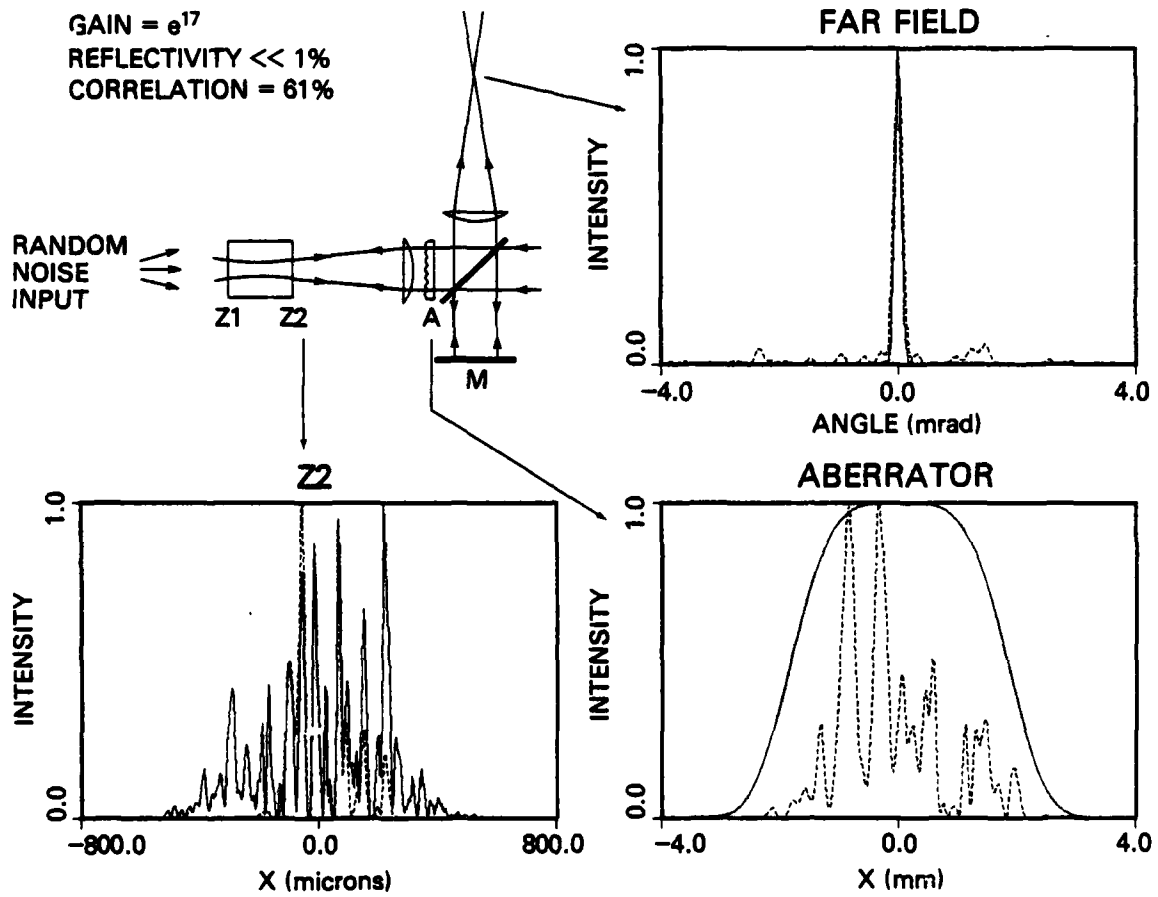


Fig. 1 - SBS phase conjugation model, showing intensity profiles of the incident light (solid lines) and backscatter (dotted lines) for the case of negligible pump depletion

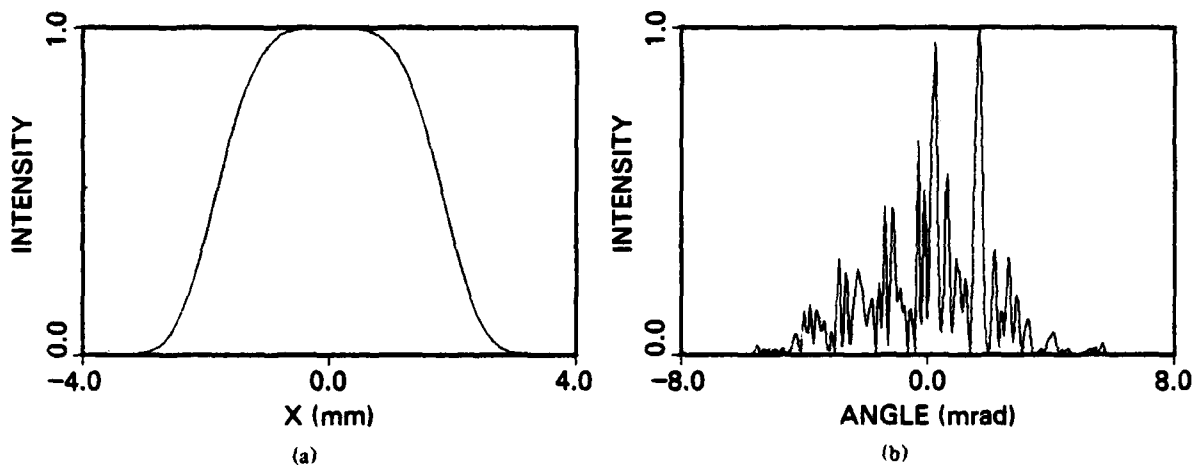


Fig. 2 — Near field (a) and far field (b) intensity profiles of the incident light after traversing the aberrator

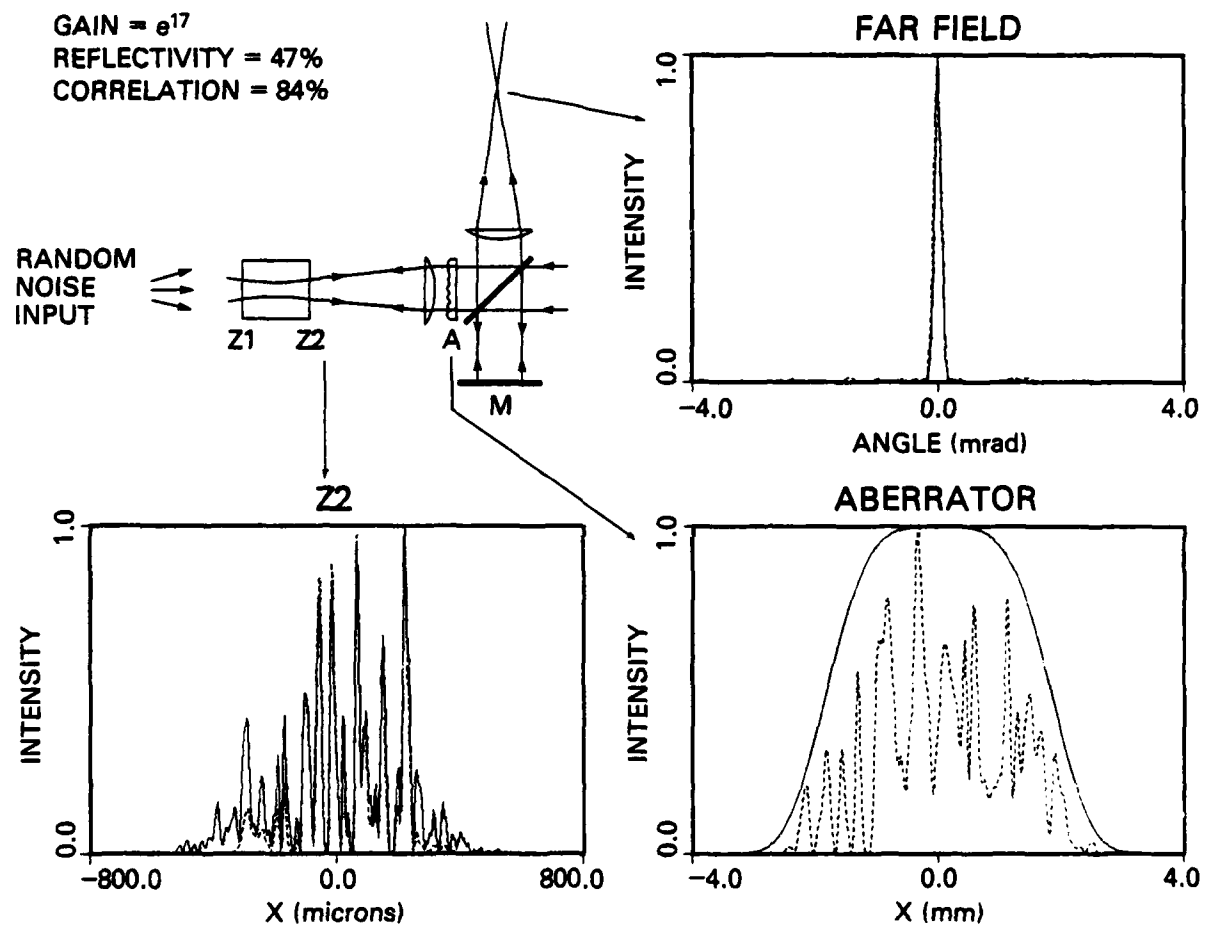


Fig. 3 — Same as Fig. 1, except for higher reflectivity, and hence pump depletion

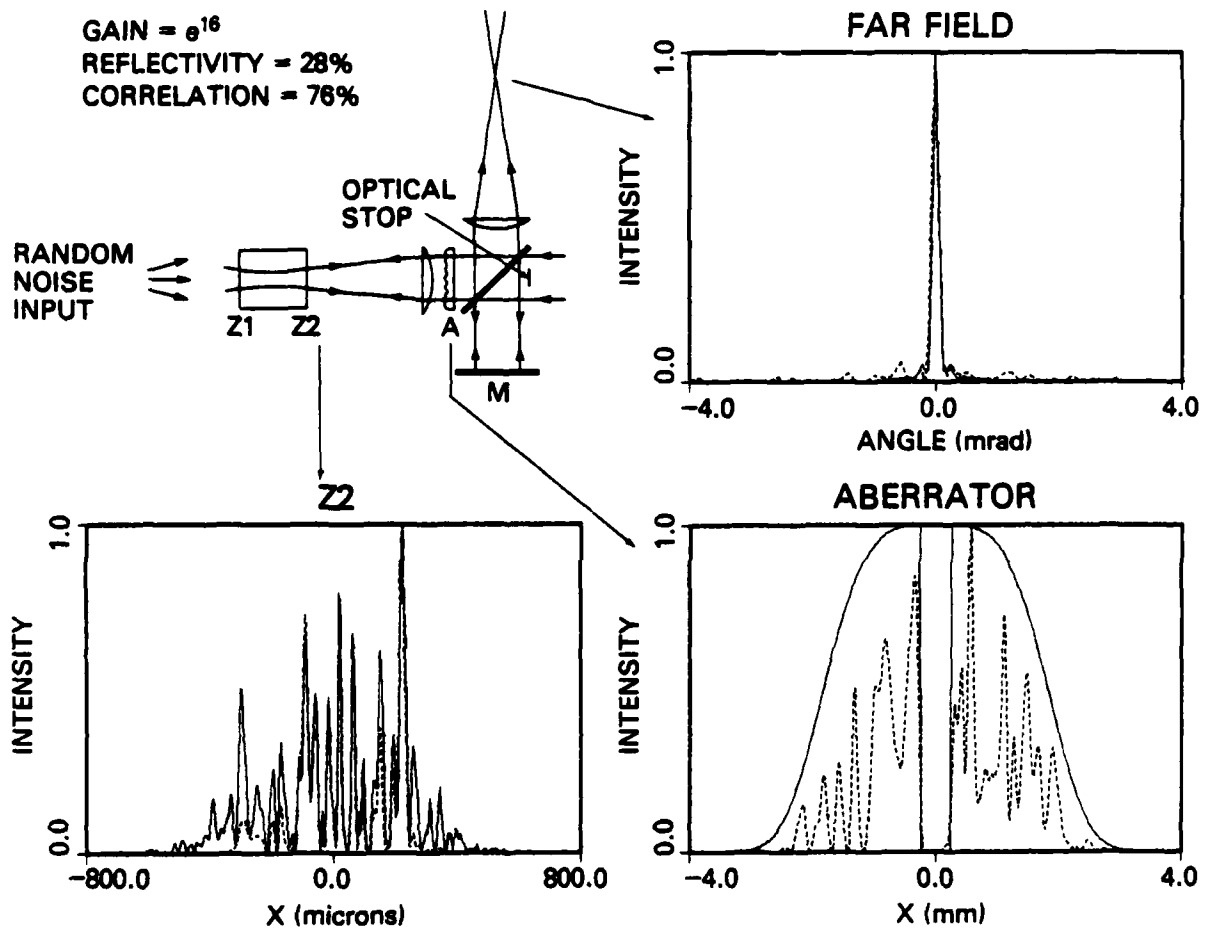


Fig. 4 - SBS phase conjugation model showing replication of an image impressed upon the incident beam